Angewandte Chemie
Eine Zeitschrift der Gesellschaft Deutscher Chemiker

Supporting Information

Twisted Aromatic Frameworks: Readily Exfoliable and Solution-Processable Two-Dimensional Conjugated Microporous Polymers

*A. Belen Marco, Diego Cortizo-Lacalle, Iñigo Perez-Miqueo, Giovanni Valenti, Alessandro Boni, Jan Plas, Karol Strutyński, Steven De Feyter, Francesco Paolucci, Mario Montes, Andrei N. Khlobystov, Manuel Melle-Franco, and Aurelio Mateo-Alonso**

anie_201700271_sm_miscellaneous_information.pdf

1. Materials and Methods

Reagents for synthesis were, if not otherwise specified, purchased from Aldrich, Fluka or Acros. Commercial chemicals and solvents were used as received. 5,6-dinitro-4,7-bis((triisopropylsilyl)ethynyl)benzo[c][1,2,5]thiadiazole[1] was synthesized according to the reported procedure.

THF, DMF and Toluene were dried using an Innovative Pure Solve solvent purification system.

Analytical thin layer chromatography (TLC) was done using aluminum sheets (20x20 cm) pre-coated with silica gel RP-18W 60 F254 from Merck.

Column chromatography was carried out using Silica gel 60 (40-60 μm) from Scharlab.

Solid-State ^{1}H and ^{13}C/CP MAS NMR spectra were recorded on a Bruker Avance III 400 MHz NMR spectrometer at a MAS rate of 12 kHz and a CP contact time of 2 ms. NMR spectra in solution were recorded on a Bruker Avance 400 MHz spectrometer at 298 K using partially deuterated solvents as internal standards. Coupling constants (*J*) are denoted in Hz and chemical shifts (δ) in ppm. Multiplicities are denoted as follows: s = singlet, d = doublet, t = triplet, m = multiplet, br = broad.

ATR-FTIR spectra were recorded on a Bruker ALPHA ATR-IR spectrometer.

Elemental analysis was carried out in a Euro EA Elemental Analyzer from EuroVector.

UV-vis-NIR were performed in a Perkin-Elmer Lambda 950 spectrometer

The pore structure was evaluated by nitrogen sorption isotherms, measured at 77 K with a Micromeritics ASAP 2020 Physisorption Analyzer. Before measurement, the samples were degassed in vacuum at 230 °C for 10 h. The Brunauer-Emmett-Teller (BET) method was used to calculate the specific surface areas.

Transmission Electron Microscopy was performed using a TECNAI G2 20 TWIN (FEI), operating at an accelerating voltage of 200 KeV in a bright-field image mode. Samples were prepared by deposition of the molten solids on a carbon film copper grid. HRTEM analysis was performed on a JEOL2100 FEG microscope. The imaging conditions

were carefully tuned by lowering the accelerating voltage of the microscope to 100 kV and reducing the beam current density to a minimum. The sample (ca. 0.1 mg) was dispersed in methanol (2 mL) using an ultrasonic bath and deposited onto a lacey carbon film coated TEM copper grid. The morphology of the film was determined by taking micrographs of 100 nm^2 areas from different regions of the specimen, and the nano scale features were imaged using high resolution imaging of 20 nm^2 areas.

The X-ray powder diffraction patterns were collected by using a PHILIPS X'PERT PRO automatic diffractometer operating at 40 kV and 40 mA, in theta-theta configuration, secondary monochromator with Cu-Kα radiation (λ = 1.5418 Å) and a PIXcel solid state detector (active length in 2θ 3.347º). Data were collected from 3 to 80° 2θ (step size = 0.026 and time per step = 0.150 s) at room temperature. An automatic divergence slit was used, giving a constant irradiated length of 4.0 mm illumination.

Thermogravimetric analysis was performed in a TGA Q500 from TA Instruments under nitrogen with a heating rate of 10 ^{o}C/min. Air was introduced at 800 ^{o}C.

All AFM measurements were performed with a Bruker MultiMode 8 microscope in tapping mode, using AC-160-TS tips from Olympus. Samples were prepared by dropcasting few drops of a H_2O/EtOH 1:1 dispersion on highly oriented pyrolytic graphite (HOPG). The solvent was allowed to evaporate prior to imaging.

The electrochemical properties have been evaluated in a three-electrode electrochemical cell using a glassy carbon (GC) rotating disk electrode (RDE, Tacussel, France) as support for the deposition of the catalyst dispersion, a SCE reference electrode and a Pt mesh auxiliary electrode. The electrochemistry work stations used for the entire characterization was a SP-300 bipotentiostat (Biologic Instruments), having an additional current booster and a built-in impedance analyser.

2. Synthesis of Aza-CMP and TIPS-CMP.

Synthesis of Aza-CMP:

To a schlenk flask with hexaketocyclohexane octahydrate (124.8 mg, 0.4 mmol) and 1,2,4,5-benzenetetraamine chlorohydrate (170.4 mg, 0.6 mmol), a mixture of dioxane/acetic acid (1:4 v/v, 20 mL) was added. The mixture was sonicated for five minutes, and subsequently degassed by three cycles of freeze-pump-thaw. Once finished the degassing process, the mixture was heated at 135 ^{o}C and stirred for 7 days under nitrogen. After this time, reaction was cooled to room temperature and filtered off, washing the resulting dark solid with water, HCl aq. 0.2N, methanol and THF. The solid was Soxhlet extracted with water (48 h), methanol (48 h), THF (48 h) and CH_2Cl_2 (48 h). The compound was then sonicated in the presence of methanol (20 minutes), THF (20 minutes), CH_2Cl_2 (20 minutes) and Et_2O (20 minutes), before being dried under vacuum at 150 ^{o}C for 24 hours, yielding **Aza-CMP** as a black solid (73 mg, 68%). SS-^{1}H-NMR (δ) (ppm): 7.24. SS-^{13}C-NMR (δ) (ppm): 170-76, 131, 111. ATR-FTIR (cm^{-1}): 3001 (C–H, st); 1597, 1508 (C=N/C=C); 1459 (C–C, st); 1354, 1216 (C–N, st). Elemental Analysis: calculated: C (63.16%), N (29.46%) H (1.77%); observed: C (54.33%), N (22.96%) H (2.54%).

Synthesis of TIPS-CMP:

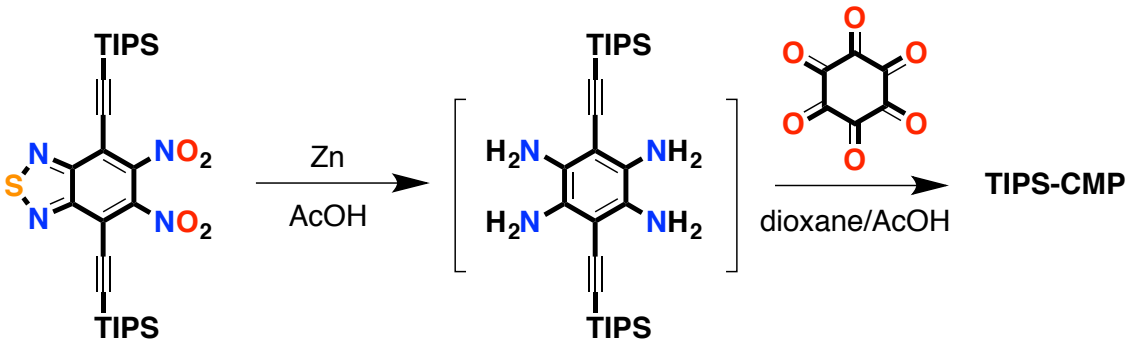

Scheme S1.

To a solution of 5,6-dinitro-4,7-bis(triisopropylsilyl(ethynyl))benzo[c][1,2,5]thiadiazole (400 mg, 0.68 mmol) in acetic acid (6 mL), zinc powder (886 mg, 13.6 mmol) was added and the mixture was stirred for 6 hours at 60 ^{o}C. After this time, reaction was cooled to room temperature and filtered off over celite, washing the solids with acetic acid (~8 mL). The filtrate was directly transferred to a Shlenk flask with hexaketocyclohexane octahydrate (71 mg, 0.68 mmol) to avoid the decomposition of

the tetraamine, and dioxane (2 mL) was added. The mixture was sonicated for five minutes, and subsequently degassed by three cycles of freeze-pump-thaw. Once finished the degassing process, the mixture was heated at 135 ^{o}C and stirred for 7 days under nitrogen. After this time, reaction was cooled to room temperature and filtered off, washing the resulting dark solid with water, HCl aq. 0.2N, methanol and THF. The solid was Soxhlet extracted with water (48 h), methanol (48 h), THF (48 h) and CH_2Cl_2 (48 h). The compound was then sonicated in the presence of methanol (20 minutes), THF (20 minutes), CH_2Cl_2 (20 minutes) and Et_2O (20 minutes), before being dried under vacuum at 150 ^{o}C for 24 hours, yielding the corresponding CMP as a black solid (41 mg, 22%). SS-^{1}H-NMR (δ) (ppm): 0.12. SS-^{13}C-NMR (δ) (ppm): 170–76 (br), 18.6, 11.9. SS-^{29}Si-NMR (δ) (ppm): –6.45. ATR-FTIR (cm^{-1}): 2940, 2861 (C–H, st); 1600, 1566, 1518 (C=N/C=C); 1454 (C–C, st); 1359, 1202 (C–N, st). Elemental Analysis: Elemental Analysis: calculated: C (69.77%), N (10.17%) H (7.93%); observed: C (49.57%), N (9.34%) H (4.27%). The observed carbon and hydrogen values are lower than the calculated on account of the formation of refractory complexes with carbon such as non-combustible silicon carbide byproducts and volatile stable silane. This behaviour has been observed for boronate ester linked COFs.[2]

3. IR Spectroscopy

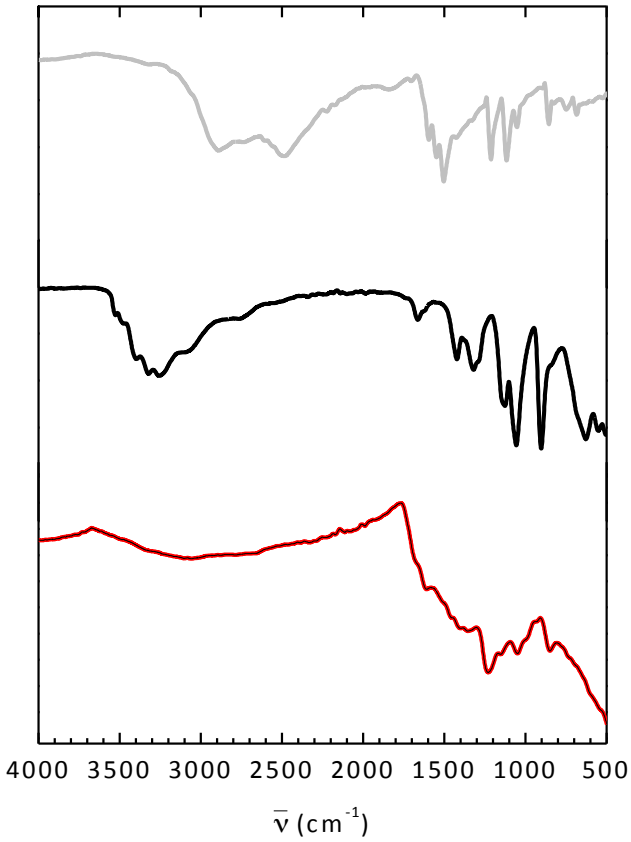

Figure S1. IR spectra of **Aza-CMP** (red) and its precursors: hexaketocyclohexane octahydrate (black) and benzenetetraamine chlorohydrate (grey).

4. Solid State-Nuclear Magnetic Resonance (SS-NMR):

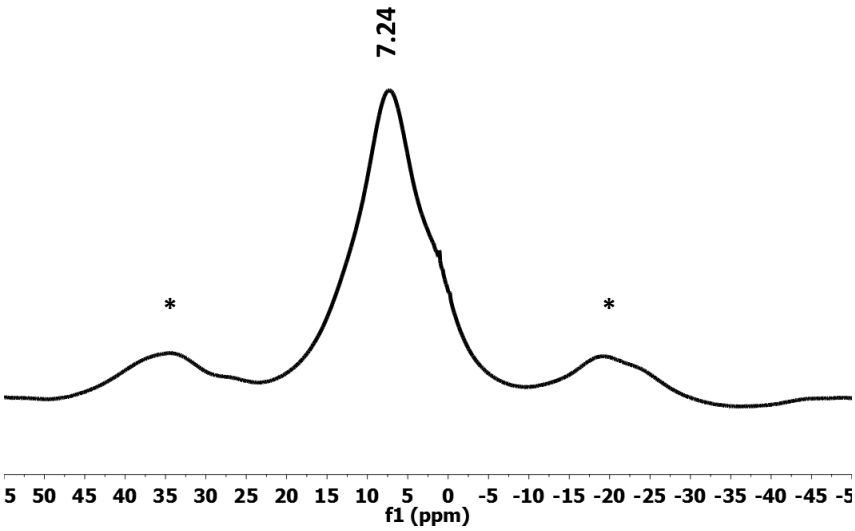

Figure S2. SS-^{1}H-NMR spectrum of **Aza-CMP**.

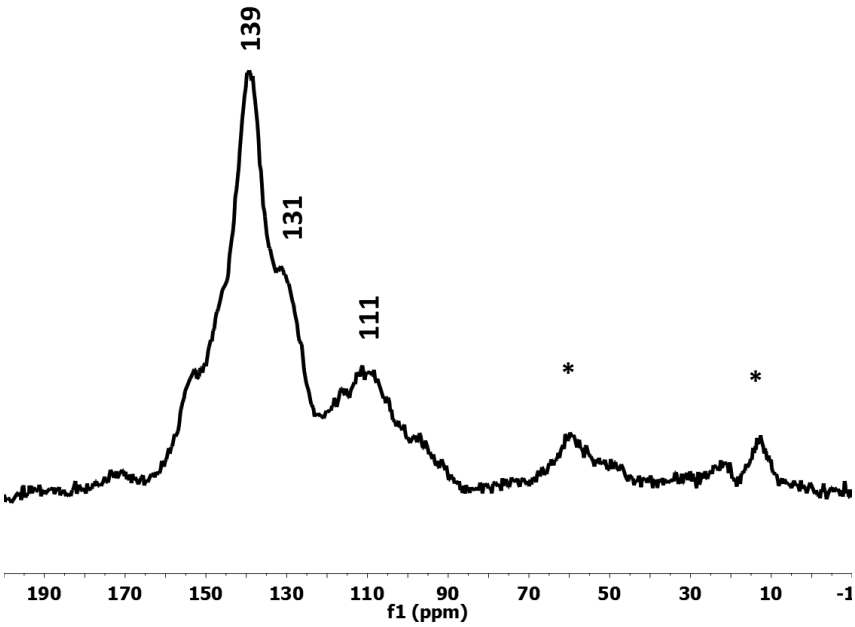

Figure S3. SS-^{13}C-NMR spectrum of **Aza-CMP**.

5. Transmission Electronic Microscopy (TEM):

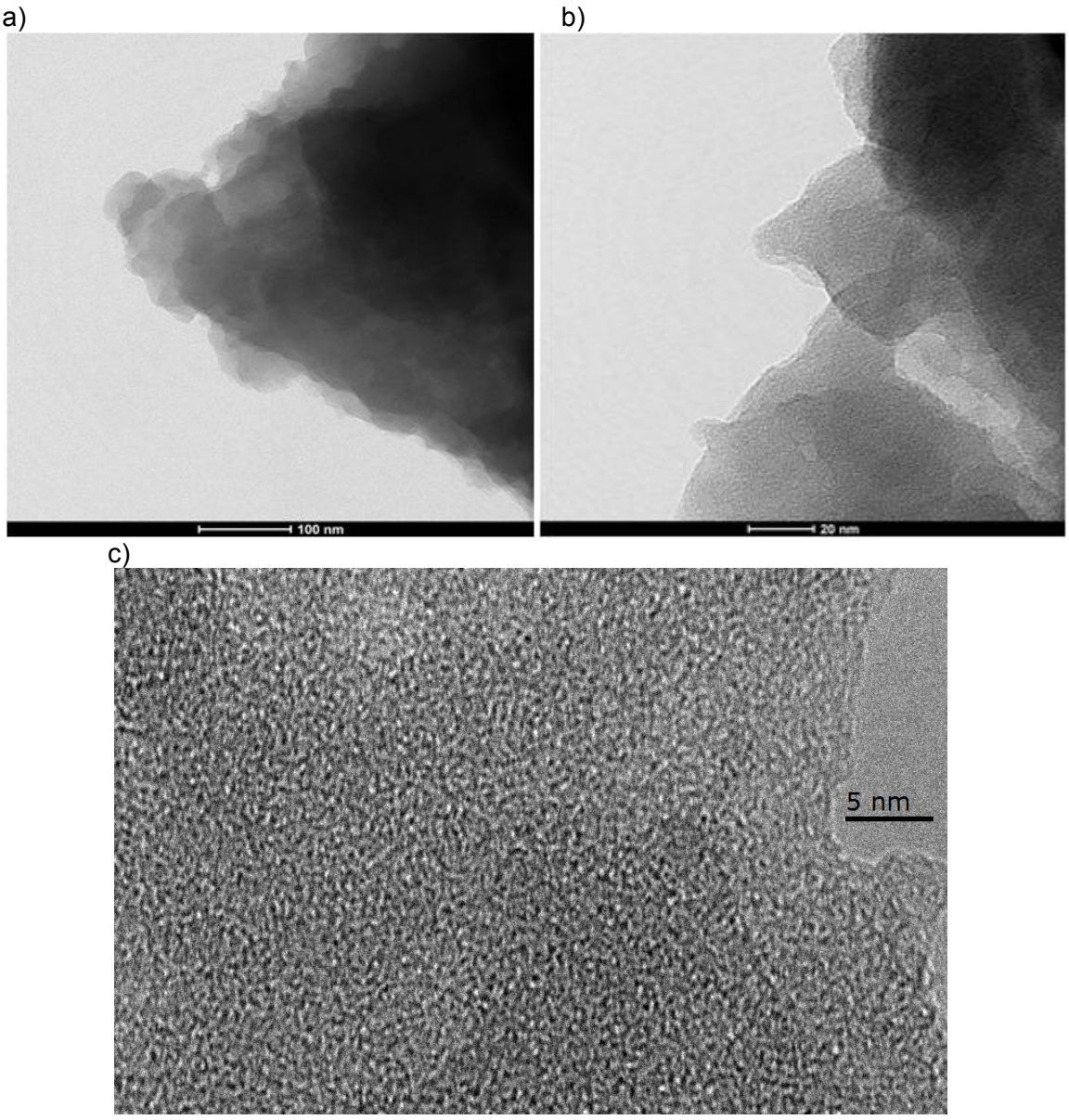

Figure S4. TEM (a and b) and and HRTEM (c) micrographs of **Aza-CMP**.

a)

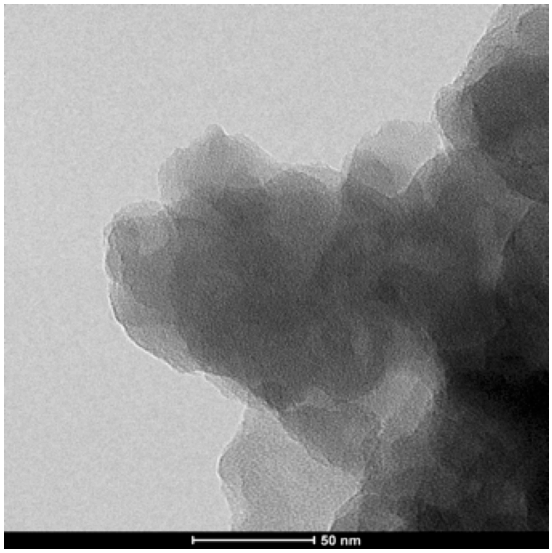

b)

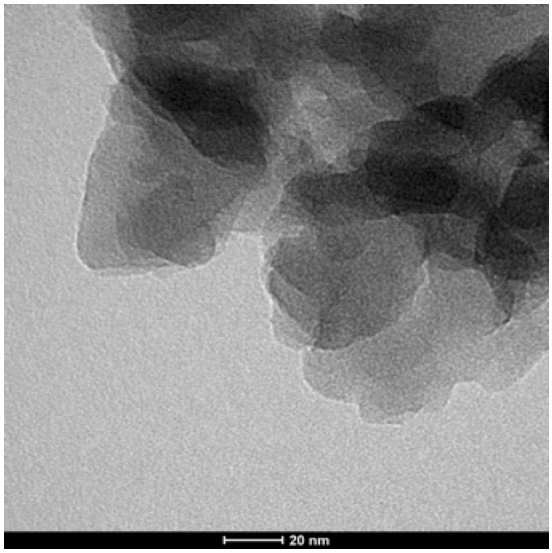

c)

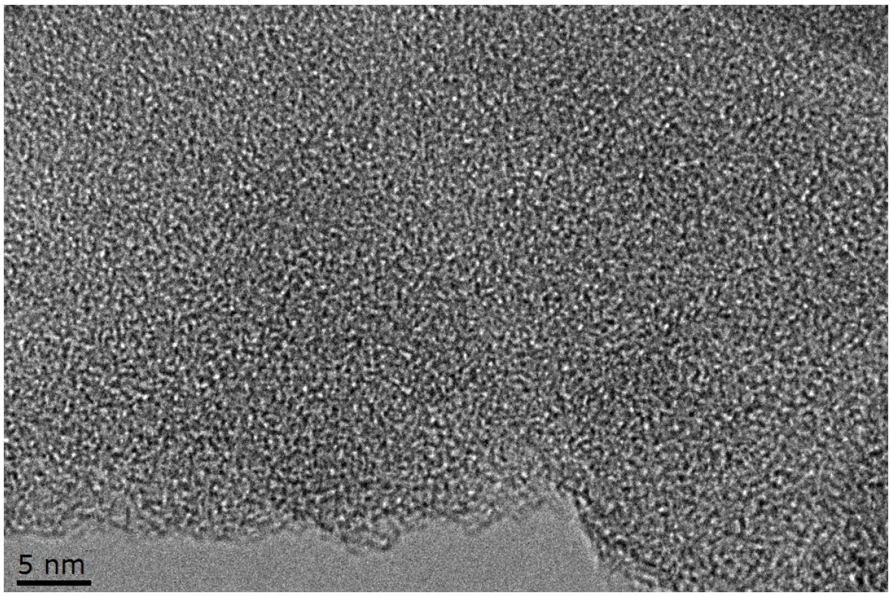

Figure S5. TEM (a and b) and and HRTEM (c) micrographs of **TIPS-CMP**.

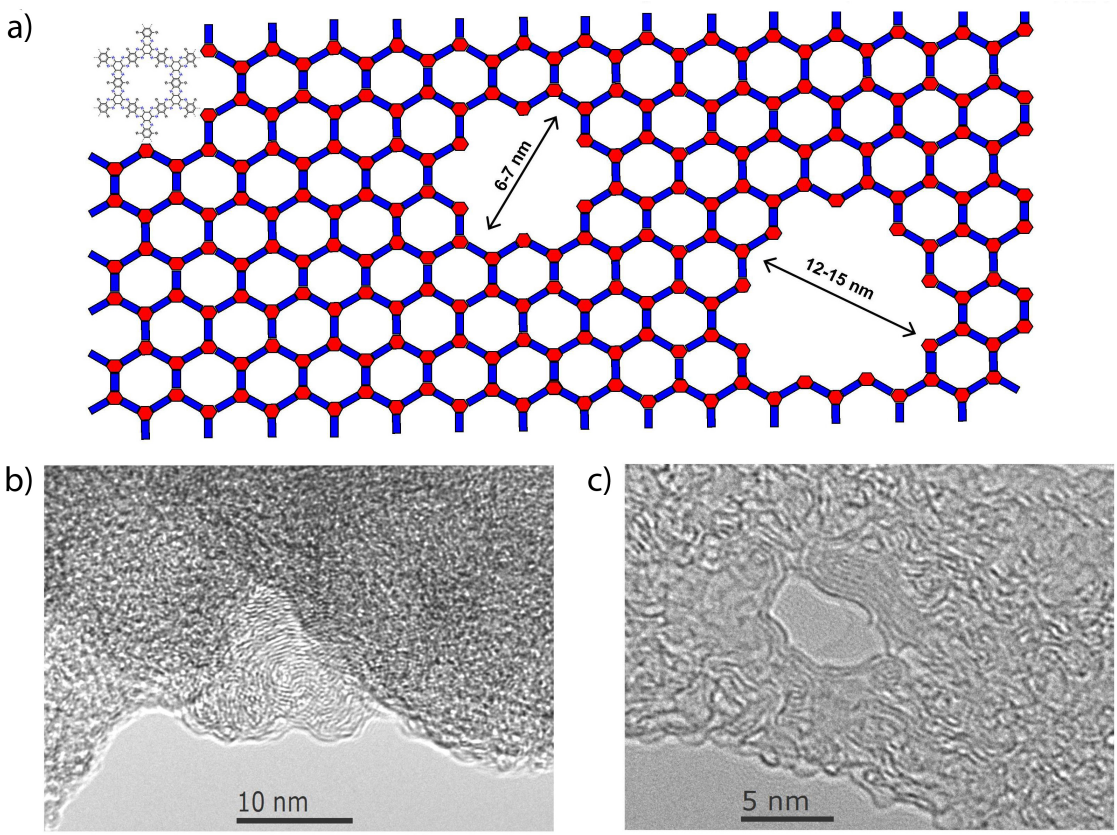

Figure S6. (a) Schematic diagram illustrating that the holes are a result of structural defects occurring in the monolayer where two or more building blocks of the hexagonal network are missing. (b and c) **TIPS-CMP**, as all covalent organic frameworks, is highly susceptible to electron beam damage during TEM imaging, such that even moderate irradiation leads to rapid degradation of the structure and transformation of **TIPS-CMP** to graphitised carbon where the graphitic layers with characteristic 0.33 nm spacing can be clearly observed.

6. Powder X-Ray Diffraction data

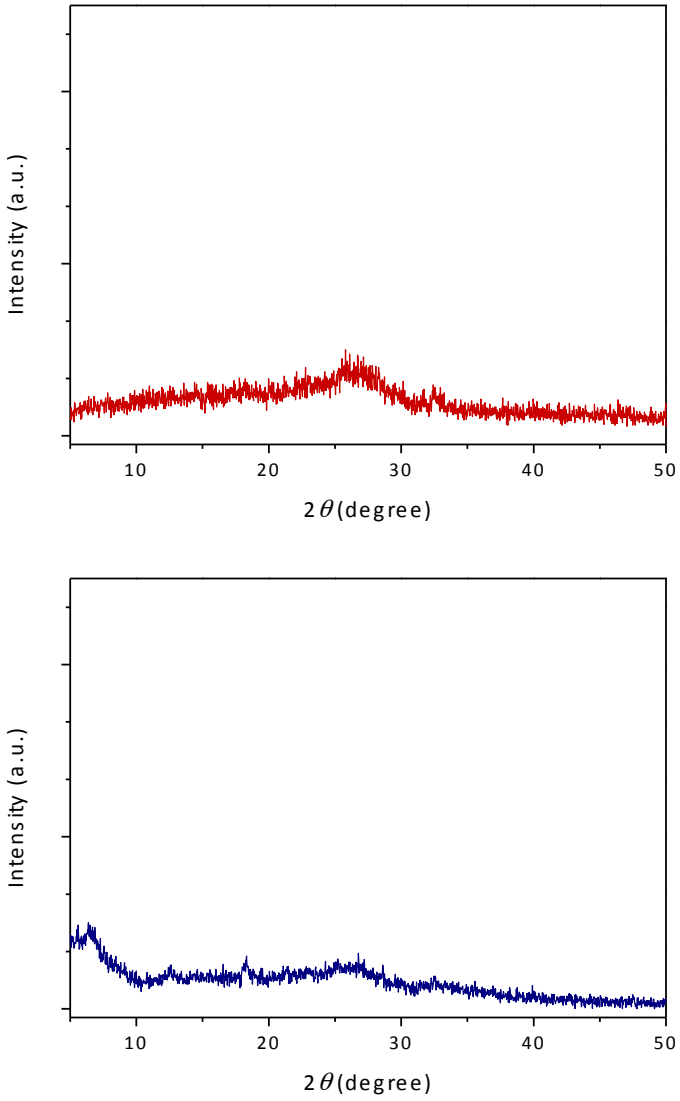

Figure S7. X-Ray powder diffraction pattern for **Aza-CMP** (top) and for **TIPS-CMP** (bottom).

7. Thermogravimetric analysis

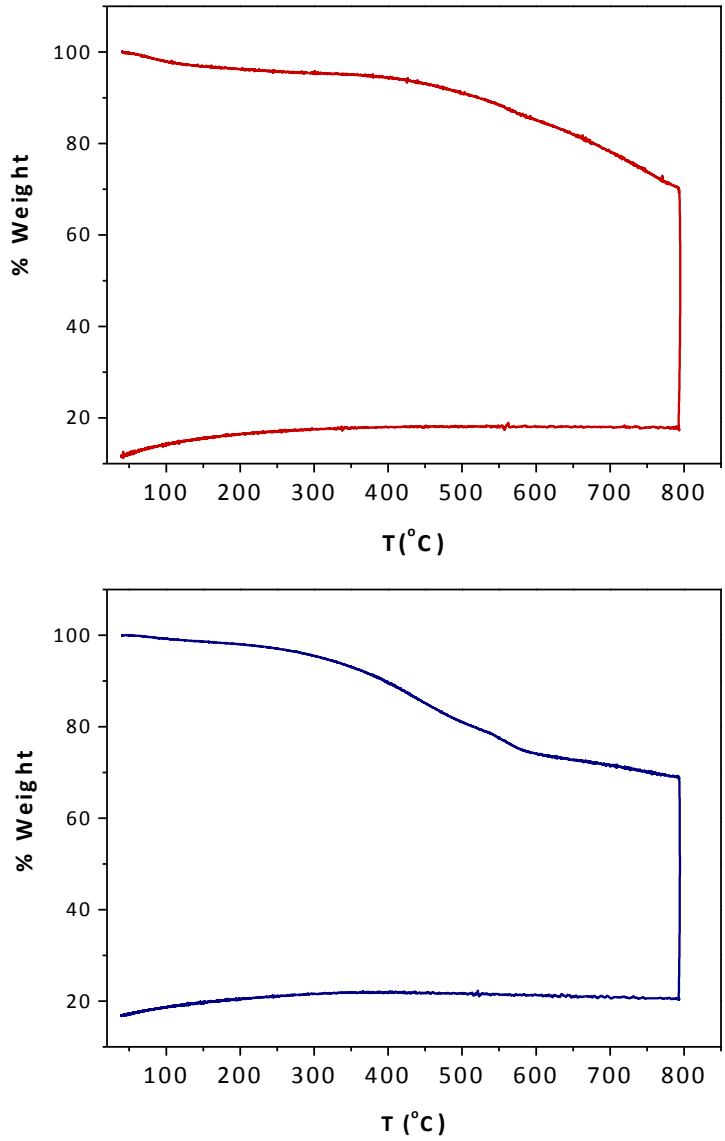

Figure S8. Thermogravimetric analysis of **Aza-CMP** (top) and of **TIPS-CMP** (bottom) performed at 10 °C/min under inert atmosphere (air was flushed after 800 °C).

8. Solubility

Solubility of CMPs was tested by adding increasing known amounts of the solids to pure trifluoroacetic acid (TFA). First, it was checked that TIPS-CMP was able to be completely dissolved in TFA in concentrations ca. 0.2 mg/mL. Then, the concentration was confirmed by adding small measured volumes of TFA until homogeneous dispersions were observed, confirming that the solubility of TIPS-CMP in TFA is 0.2 mg/mL. This process was repeated at least 10 times with reproducible results.

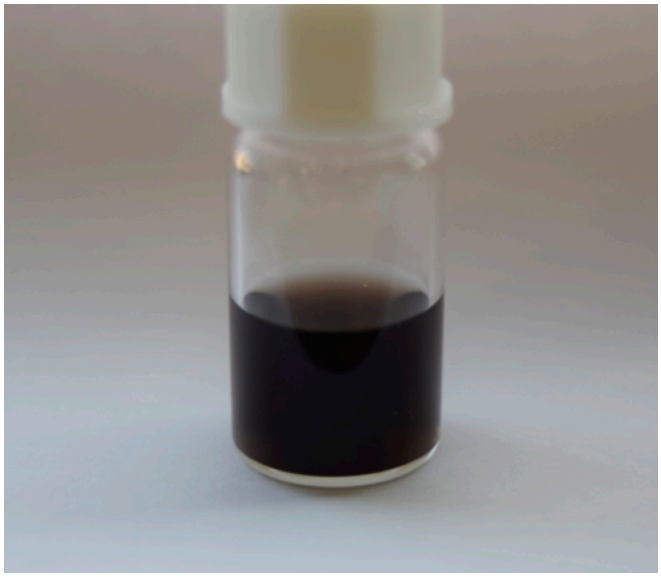

Figure S9. High-resolution picture of the TFA dispersion (0.2 mg/mL) of **TIPS-CMP**.

9. AFM studies.

0.4 mg of TIPS-CMP were sonicated in 1 ml of H_2O/EtOH (50:50) for 5 minutes and the solution started coloring black, indicating exfoliation of the flakes. The solution was sonicated for 30 minutes before dropcasting on a preheated HOPG sample (100°C) and dried for 1 minute. This sample was analysed with AFM. The size of the flakes was characterized measuring the area of individual flakes in large-scale phase images. In total, the area of 84 individual flakes was measured and the area distribution is presented in the diagram in figure S10. From this diagram, we can see that the largest fraction of flakes is that with the smallest area (up to 12000 nm²).

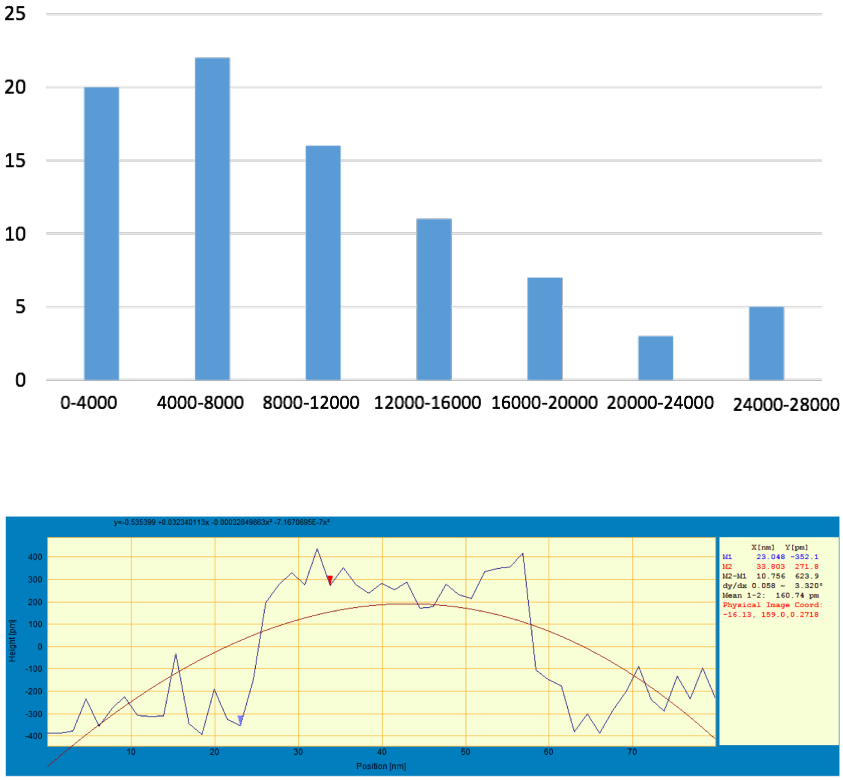

Figure S10. Size distribution of TIPS-CMP in an EtOH/water 1:1 dispersion divided in 4000 nm² intervals (top). Height estimation of an individual flake on bare HOPG (bottom).

10. Thin film deposition

Thin films of **TIPS-CMP** were prepared by drop casting a solution 0.15 mg/mL in a mixture DMF/TFA 95:5 v/v on a glass slide, and were left to dry under air in a protected environment and subsequently under vacuum to assure evaporation of DMF before recording the electronic absorption spectra.

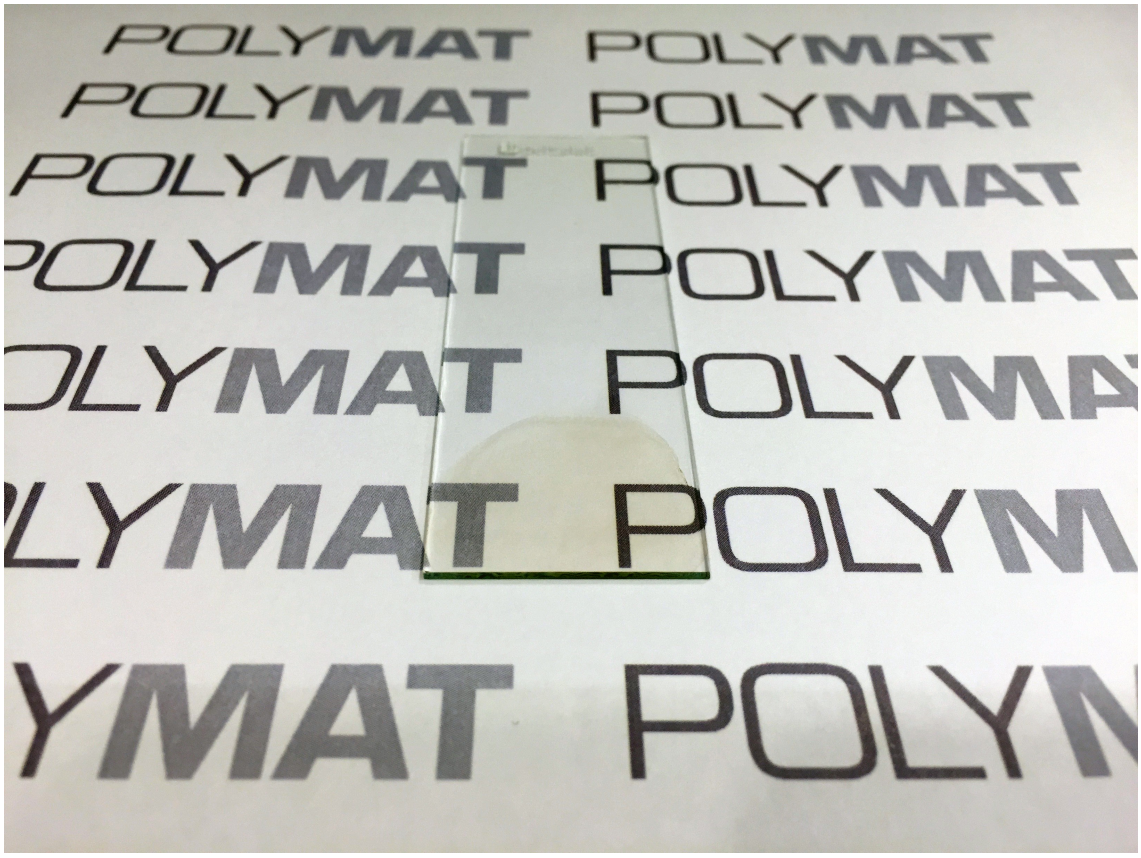

Figure S11. High-resolution pictures of the thin films prepared by drop casting a 0.15 mg/mL solution of **TIPS-CMP** in DMF:TFA 95:5 on a glass substrate.

11. Theoretical calculations

Computer models of the TIPS-CMP 2D-extended system were performed in all cases with a molecular analogue with the empirical formula $C_{372}N_{36}Si_{24}H_{516}$ containing one hexagonal pore. Three-dimensional structures were generated with the program Avogadro 1.1.1.[3] and optimized with the program MOPAC2012[4] with the PM6-DH2 semiempirical Hamiltonian.[5] Due to the large size of the molecular analogue, 948 atoms, structural simulation studies were performed with semiempirical models benchmarked against previously studied twisted molecules.[6] Different semiempirical Hamiltonians were tried, namely: AM1, PM6, PM6-DH2 and PM7, and compared with the X-ray structure and DFT models of *twisted*-HATNA. PM6-DH2 was chosen as it yielded an average twist angle between blades of 65° in better agreement with the experimental value (67°) than DFT (63°).[6]

Conformational search

In order to explore different conformations, we performed Molecular Dynamics (MD) simulations at 298 K with the molecular mechanics MMFF94 force field as implemented in the software Tinker. Collisions with solvent molecules were considered implicitly through the use of stochastic dynamics with a friction coefficient of 2 ps^{-1} to improve conformational sampling. The simulation was run for 1 ns and snapshots of the trajectory were selected at 20 ps intervals yielding 50 different conformations that were optimized at the PM6-DH2 level. All conformations in the MD simulation look very much alike and the TIPS functional groups show similar relative orientations with respect to the aromatic core (Table S1).

The “best minimum” (Table S1) corresponds to the conformer with the lowest energy at the PM6-DH2 level and shows twisting angles similar to the average values for all conformers. The table shows also the maximum and minimum relative angles and the Standard Deviation (SD) for all conformations.

The average of the average twisting angles for each conformations is shown in Table S2. The average twisting angle for each conformer oscillates between 68 (minimum) and 77 (maximum) degrees.

Table S1. Angles between adjacent branches in the inner pore (the change of sign implies that the dihedral angles are antiparallel, i.e. the branches are pointing in alternating, up and down, directions).

		angle 1	angle 2	angle 3	angle 4	angle 5	angle 6
Best minimum	1 conformer	72	-95	65	-63	90	-74
Statistics 1 ns/20 ps	Average all conformers	70	-92	60	-57	89	-70
Statistics 1 ns/20 ps	Maximum all conformers	87	-99	74	-74	101	-78
Statistics 1 ns/20 ps	Minimum all conformers	56	-84	47	-45	78	-58
Statistics 1 ns/20 ps	SD all conformers	6	4	7	7	5	4

Table S2. Average angles between adjacent branches in the inner pore.

Statistics 1 ns/20 ps	Average |angle|	73
Statistics 1 ns/20 ps	Max. ave. |angle|	77
Statistics 1 ns/20 ps	Min. ave. |angle|	68
Statistics 1 ns/20 ps	SD |angle|	2

Ab-initio DFT calculations

We computed the frontier orbitals energies at the B3LYP-631g(d,p) level of the aromatic core of a pore in two conformations: a twisted, **TIPS-CMP**, conformation (partial optimization) and a flat, **Aza-CMP**, conformation (full optimization). In addition, the ***twisted*-HATNA** properties calculated at the same level are presented for comparison (Table S3).

Table S3. B3LYP-631g(d,p) calculated electronic properties (all energies are in eV).

	LUMO+2	LUMO+1	LUMO	HOMO	HOMO-1	HOMO-2	gap
TIPS-CMP Twisted aromatic core	-3.66	-3.67	-3.77	-5.82	-5.83	-5.85	2.1
Aza-CMP Flat (D_{6h}) aromatic core	-3.71	-3.71	-3.81	-5.83	-5.83	-5.83	2.0
***twisted*-HATNA**	-2.62	-2.63	-2.98	-5.82	-5.87	-5.87	2.8

Adsorption on graphite

The adsorption of TIPS-CMP on graphite surfaces was studied using the molecular analogue adsorbed on monolayer graphene (Figure S13). In order to allow for the molecule to relax on the surface we performed Molecular Dynamics (MD) simulations at 298 K and 500 K with the molecular mechanics MMFF94 force field using a home version of the software Tinker. Stochastic dynamics with a friction coefficient of 2 ps^{-1} was used to improve conformational sampling. Simulations were run for 1 ns, after which the final conformations were optimized with MMFF94. Standard MMF94 parameters overestimate the intermolecular distances in π-π systems,[6b] to account for this the adsorbed geometries were also optimized using van der Waals MMFF94 parameters "corrected" to reproduce accurately the molecular geometry of the benzene dimer.[6b] The average height of the atoms in the adsorbate molecules with respect to the surface for all models are summarized in table S4.

Table S4. Average heights for the molecular analogue of TIPS-CPM on graphene with different force field parameters.

Standard MMFF94, MD T=298 K	8.04 Å
Standard MMFF94, MD T=500 K	8.11 Å
Corrected MMFF94, MD T=298 K	7.72 Å
Corrected MMFF94, MD T=500 K	7.83 Å

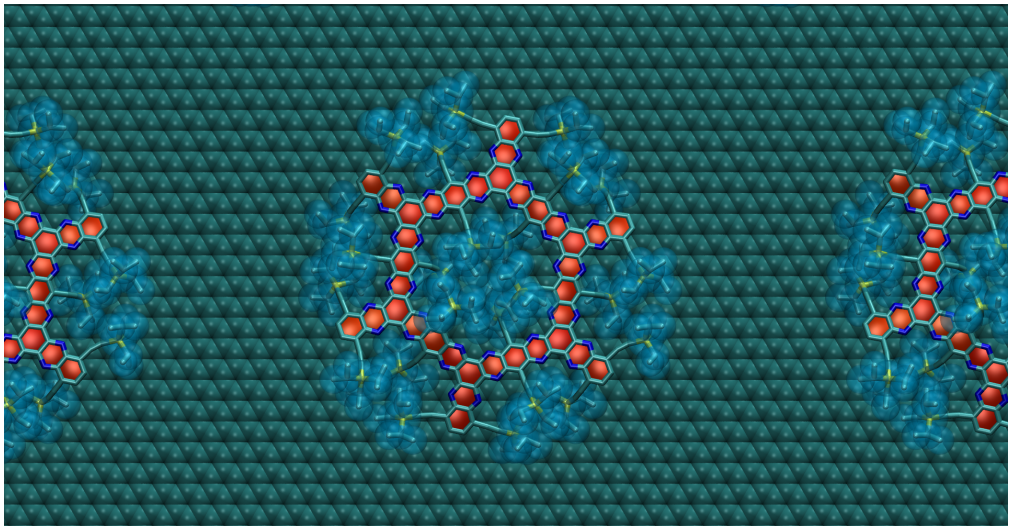

Figure S12. Top view of a TIPS-CPM molecular analogue adsorbed on graphene. Only C (light blue), N (dark blue), and Si (yellow) atoms are rendered. The aromatic rings are emphasized in red, while the C atoms in TIPS groups are rendered as semi-transparent spheres. Structure computed by geometry optimization with corrected MMFF94 parameters from an MD simulation at 298 K.

12. Catalytic activity for the Oxygen Reduction Reaction (ORR)

To evaluate the catalytic ability of **TIPS-CMP** for the Oxygen Reduction Reaction (ORR), a GC electrode was covered by dropcasting with a suspension 0.2 mg/mL in TFA, depositing a total amount of 50 µL (catalyst loading of 140 µg/cm^2). Thus prepapared modified electrodes were used as working electrodes in the ORR experiments in ultrapure KOH 0.1M at a scan rate of 10 mVs^{-1}.

Koutecky-Levich analysis. By representing the limiting current of ORR (at a certain potential) as a function of the rotation speed, the number of electrons involved in the ORR process can be estimated by the slope of the fitting line with Equation S1:

$$n = \frac{1}{0.62\, b\, F A C_0 D^{2/3} v^{-1/6}}$$

Equation S1.

Where F is the Faraday constant (96500 C), C_0 is the oxygen concentration in KOH (8.4x10^{-7} mol/cm^3), A is the electrode surface area (0.07 cm^2), D is the diffusion coefficient (2x10^{-5} cm^2 s^{-1}) and *v* kinematic viscosity (0.008977cm^{2}s^{-1}).[7]

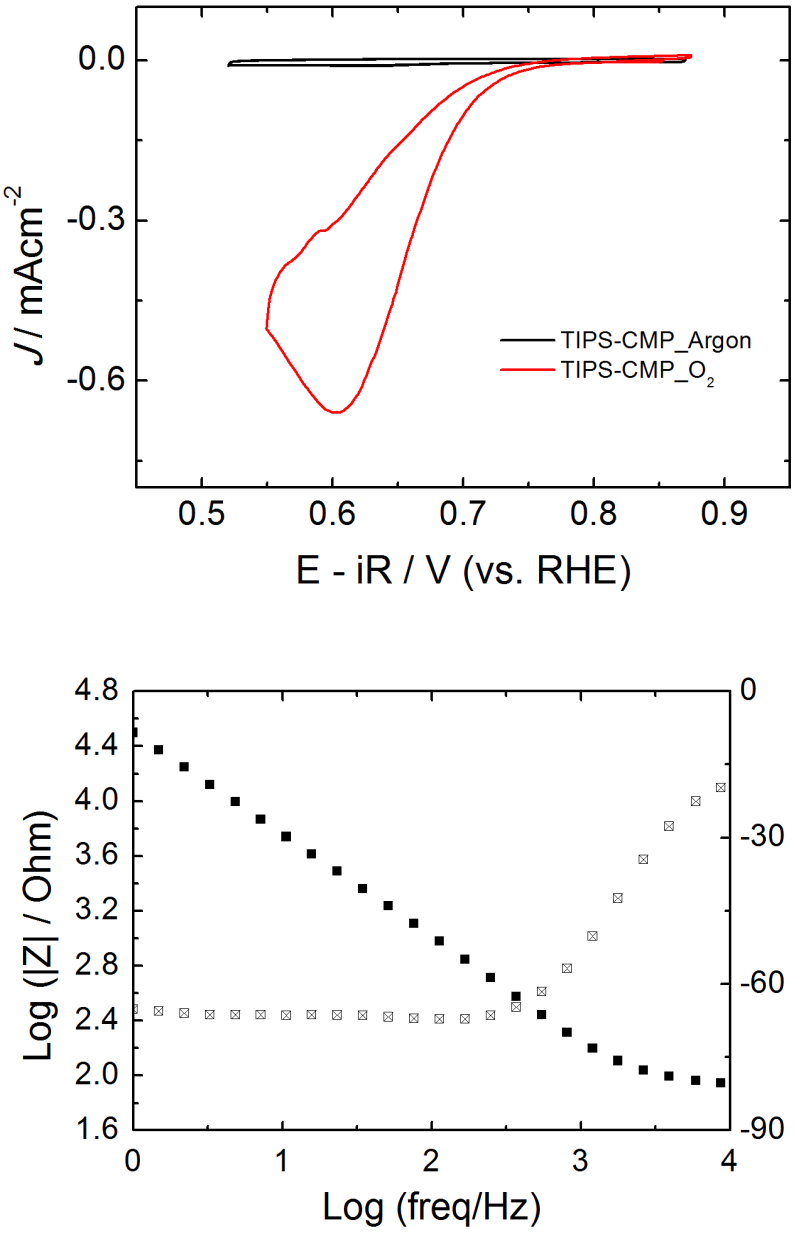

Figure S13. (Top) Representative cyclic voltammogram for **TIPS-CMP** in Ar (black line) and O_2-saturated (red line) KOH 0.1 M. Electrode without rotation. Scan rate: 50 mV/s. (Bottom) Impedance measurements for the determination of solution resistance.

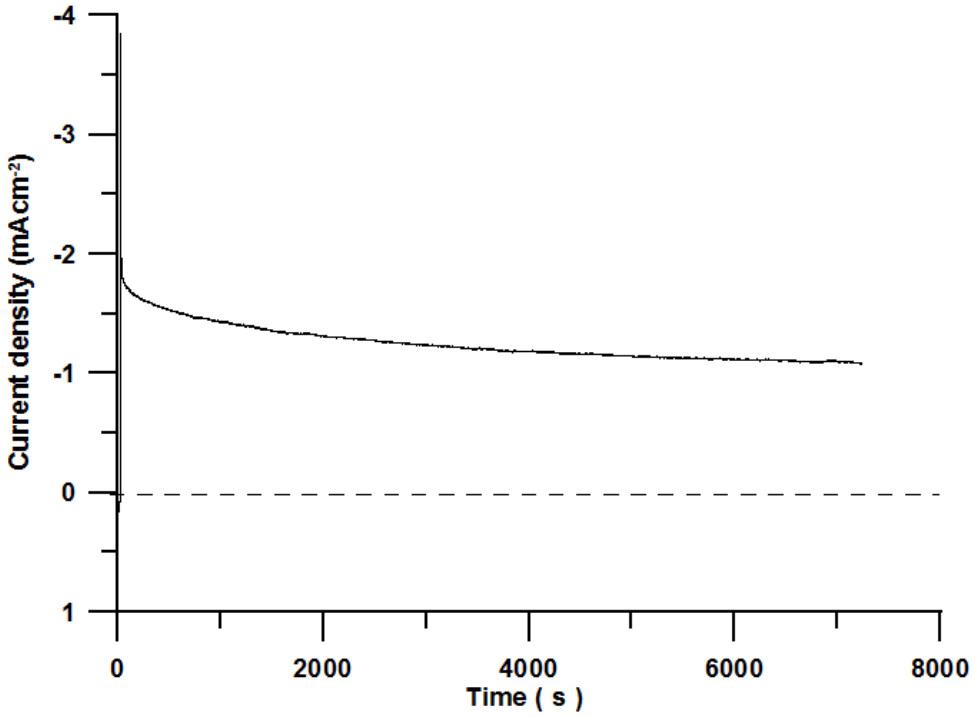

Figure S14. Potentiostatic electrolysis at *E* = 0.6 V_{RHE} for **TIPS-CMP**-casted for O_2-saturated in aqueous ultrapure 0.1 M KOH (rotating speed 1600 rpm).

13. References.

1. A. B. Marco, D. Cortizo-Lacalle, C. Gozalvez, M. Olano, A. Atxabal, X. Sun, M. Melle-Franco, L. E. Hueso, A. Mateo-Alonso, *Chem Commun.,* **2015**, *51*, 10754–10757.
2. a) Côté, A. P.; Benin, A. I.; Ockwig, N. W.; O'Keeffee, M.; Matzger, A. J.; Taghi, O. M. *Science* **2005**, *310*, 1166–1170; b) Spitler, E. L.; Koo, B. T.; Novotney, J. L.; Colson, J. W.; Uribe-Romo, F. J.; Guitierrez, G. D.; Clancy, P.; Dichtel, W. R. *J. Am. Chem. Soc.* **2011**, *133*, 19416–19421.
3. M. D. Hanwell, D. E. Curtis, D. C. Lonie, T. Vandermeersch, E. Zurek, G. R. Hutchison, *J. Cheminform*. **2012**, *4*, 17.
4. J. D. C. Maia, G. A. Urquiza Carvalho, C. P. Mangueira, S. R. Santana, L. A. F. Cabral, G. B. Rocha, *J. Chem. Theory Comput.* **2012**, *8*, 3072–3081.
5. a) M. Korth, M. Pitoňák, J. Řezáč, P. Hobza, *J. Chem. Theory Comput.* **2010**, *6*, 344–352; b) K. Strutyński, J. A. N. F. Gomes, M. Melle-Franco, *J. Phys. Chem. A*, **2014**, *118*, 9561–9567.
6. S. Choudhary, C. Gozalvez, A. Higelin, I. Krossing, M. Melle-Franco, A. Mateo-Alonso, *Chem. Eur. J.*, **2014**, *20*, 1525–1528.
7. Davis, R. E.; Horvath, G. L.; Tobias, C. W. *Electrochim. Acta* **1967**, *12*, 287–297.